

Probabilistic seismic response of inelastic building foundation systems

Enrique Bazán-Zurita & Iván Díaz-Molina
Paul C. Rizzo Associates, Pittsburgh, Pa., USA

Jacobo Bielak
Carnegie Mellon University, Pittsburgh, Pa., USA

Norma C. Bazán-Arias
University of Pittsburgh, Pa., USA

ABSTRACT: This paper quantifies the importance of uncertainties in the input ground motion and in the dynamic properties of structural systems on the peak response of building-foundation systems, for structures resting on both firm ground and on sites where soil-structure interaction effects are significant, with special emphasis on Mexico City.

1 INTRODUCTION

The two primary sources of uncertainty in the seismic response of structural systems are the random nature of earthquakes and the statistical variations of the dynamic properties of the structural components. The main objective of this study is to gain a better understanding of the impact on uncertainties of the inelastic behavior of building-foundation systems under earthquake excitation by means of simple models. The present study is motivated primarily by the extensive damage experienced by buildings located in the lakebed region of Mexico City during the 19 September 1985 earthquake. Since the lakebed consists primarily of very deformable silty clay deposits, it is of interest to examine the effects that soil-structure interaction (SSI) might have had on structural response, and to compare it to the response of structures supported on more competent soils that can be idealized as fixed base. Also, consideration of inelastic effects becomes crucial due to the long duration and long dominant period of the excitation, and to the amplification of the incoming seismic motion by the soft soil deposits.

In pursuing this objective, we have conducted a parametric study of an idealized single-story plane model, meant to represent the "fundamental mode" response of actual buildings, using two prototype foundation conditions: one very stiff (fixed base) and the other simulating conditions in Mexico City. The basic free-field surface excitation is given by the EW component of the surface acceleration recorded at SCT during the 1985 earthquake, hereinafter referred to as the SCT-85 record. We focus our attention on two response quantities that are often related to damage, namely, ductility demand and interstory drift of the structure.

2 FORMULATION

The system under investigation is shown in Figure 1. It consists of an elastoplastic hysteretic viscously damped structure with one degree-of-freedom whose properties

represent the "fundamental mode" of a multistory building. This structure rests on a foundation assumed to be rigid and embedded in a viscoelastic halfspace, with no slippage allowed between the base and the soil. Formulated thus, the system has three significant degrees of freedom, namely, horizontal translation of the top mass, m_1 , with respect to the foundation, horizontal translation of the base mass relative to free field motion, and rotation of the system in the plane of motion.

If there is no interaction, the relevant properties of the superstructure are: the fixed-base fundamental period, T , the damping ratio, ζ , and the ratio of the yield force, f_y , to the weight of m_1 . When SSI is significant, the relevant foundation parameters are its mass, m_0 (or the ratio m_0/m_1), the SSI translational (horizontal) and rotational stiffness, k_v and k_0 , of the foundation, and the translational and rotational SSI damping ratios, ζ_v and ζ_0 . In addition, some geometric parameters become relevant: the radius of gyration of the masses, the aspect ratio defined as the building height H over the base mat dimension L , and the ratio of the embedment depth, E , to H . We have considered that the base mat is square and that the effective height of the equivalent single-story representing the first mode of the superstructure (see Figure 1) is $h_1=0.75H$.

For a given fixed-base period the best estimate of the superstructure stiffness, k , is $4\pi^2 m_1 / (T)^2$. Then, the best estimates of k_v and k_0 are defined to satisfy the following equations:

$$k_0 = \beta k_v L^2$$

$$(T'/T)^2 = 1 + k/k_v + k h_1^2/k_0$$

The last equation is proposed by Jennings and Bielak (1973) to estimate the SSI period T' . In this study, we have considered that T'/T and β are constant and equal

to 1.25 and 0.27, respectively. It also has been assumed that m_0 is 1/6 of m_1 and that E/H is the same as m_0/m_1 . The best estimate values adopted for the damping ratios are $\zeta=0.05$, $\zeta_v=0.30$, and $\zeta_0=0.10$.

To represent the seismic design process, f_y was calculated as the spectral ordinate for ductility demand equal to 4 times the weight of m_1 . The following three cases were considered: 1) fixed based systems, with f_y corresponding to the fixed base period, T , 2) SSI systems case A, with f_y calculated with the spectral value corresponding to the SSI period, T' , and 3) SSI systems case B, with the same f_y as for the fixed-base case. The design spectrum is taken to be the SCT-85 record for 5 percent damping ratio and ductility equal to 4. This spectrum as well as the elastic spectrum for 5 percent damping are shown, on Figure 2. The elastic design spectrum and the spectrum for ductility equal to 4 prescribed by the Mexico City Code (1987) are also depicted on Figure 2. Additional damping resulting in the first mode of the SSI system as a result of the relatively high damping ratio in the foundation is not incorporated in our design procedure.

Once the system properties have been established, one needs to solve a system of three nonlinear differential equations of motion due to the inelastic element representing the restoring force in the superstructure. These equations were solved numerically by the Newmark constant acceleration step-by-step procedure.

3 EFFECT OF VARIABILITY IN THE INPUT GROUND MOTION

The random nature of earthquakes is incorporated into the analysis by using as seismic input an ensemble of 13 synthetic acceleration time histories that simulate events similar to the 1985 earthquake in Mexico City (Grigoriu et al., 1988). Figure 3 compares pseudo acceleration spectra of the synthetic records with that of the SCT-85 record. Note that all records have a very similar frequency content and that the mean spectrum for simulated records matches very closely the SCT-85 spectrum.

Only systems with a fixed-base period between 0.4 and 4.0 seconds were included in this study, as this covers the practical range of interest. As stated in the previous section, fixed-base and SSI (cases A and B) systems were designed with the SCT-85 spectrum for ductility demand of 4. Then, dynamic analyses of each system, and for each case, were performed using the 13 synthetic records.

Figure 4 shows mean ductility demands for the three design cases. Values for selected periods are also presented in Table 1. For fixed-base and the SSI case B the mean ductility demands are close to or smaller than the target value of 4, for periods of 1.2s and longer. For SSI case A, however, the mean ductilities are higher in the same range of periods. In all cases, very high mean ductilities result for small periods; in particular, for $T = 0.4s$, values as high as 18 are obtained.

Table 1. Effect of input motion variability on ductility demand

period (seconds)	best estimate	mean	σ
Fixed-Base			
0.4	3.8	10.0	13.9
1.2	4.0	3.8	2.0
2.0	4.0	3.6	0.9
2.8	4.0	4.3	0.9
3.6	3.9	4.5	1.1
SCT-85SSI Case A			
0.4	3.4	15.6	20.5
1.2	4.3	5.9	2.6
2.0	5.5	4.5	1.3
2.8	5.9	5.8	1.5
3.6	5.7	8.2	2.4
SSI Case B			
0.4	19.0	18.3	22.2
1.2	4.1	5.4	2.3
2.0	3.5	3.1	1.0
2.8	3.8	3.6	0.9
3.6	3.6	4.1	1.3

Figure 5 compares mean ductility demands for the synthetic records with the results for the SCT-85 record, for SSI case A systems. From this figure and from Table 1, it can be seen that the mean ductilities are higher than the SCT-85 values for all periods except 2s. The larger differences occur at $T = 0.4s$, in which the SCT-85 value is only 22 percent of the mean ductility. Figure 5 also shows the mean ductility demands plus one standard deviation. Large dispersions occur at $T = 0.4s$, and remain significantly smaller and uniform for other periods.

Figure 6 presents mean interstory drifts for the three cases. Selected results are also listed in Table 2. In general, the inclusion of SSI produces an increase in the interstory drift for periods smaller than 1.6s and a reduction for longer periods. The differences, however, are not as noticeable as in the mean ductility demands. Figure 7 compares mean interstory drifts for the synthetic records with those corresponding to the SCT-85 record, for SSI case A models. Observe that the mean values are higher than the SCT-85 drifts for periods smaller than 1.6s, with the larger differences again at $T = 0.4s$. Figure 7 also shows the mean interstory drifts plus one standard deviation. Large dispersions occur for periods smaller than 1.6, and are significantly smaller and more uniform for longer periods.

Figure 8 is a plot of the cumulative probability of the 13 ductility demands for the fixed-base case with $T=2s$. The vertical scale is doubly logarithmic. In this format, a variable having a Gumbel Type I probability distribution (Gumbel, 1958) appears as a straight line. Figure 8 indicates that this distribution constitutes a

Table 2. Effect of input motion variability on interstorey drift (times 10^{-3})

period (sec)	SCT-85	mean	σ
Fixed-Base			
0.4	2.4	8.9	10.6
1.2	8.0	7.8	4.1
2.0	10.3	9.9	4.0
2.8	6.2	6.7	1.4
3.6	4.4	5.1	1.2
SSI Case A			
0.4	2.3	10.7	14.1
1.2	7.8	10.7	4.7
2.0	11.0	8.9	2.6
2.8	5.9	5.7	1.5
3.6	3.3	4.8	1.4
SSI Case B			
0.4	12.2	11.7	14.2
1.2	8.2	10.6	4.5
2.0	9.0	8.2	2.6
2.8	6.0	5.7	1.4
3.6	4.0	4.6	1.4

Table 3. Variability bounds for system parameters.

Variable	lower bound best estimate	upper bound best estimate
m_1/m_0	0.90	1.10
k, ζ	0.70	1.30
f_y	0.85	1.45
k_v	0.50	1.50
β	0.90	1.10
ξ_0, ξ_v	0.70	1.30

reasonable fit to the statistical results. Similar fits were observed for ductilities at other periods and for interstorey drifts. This allows one to calculate exceedance probabilities for prescribed values of the response.

4 EFFECT OF VARIABILITY IN SYSTEM PROPERTIES

To study the effect of the variability of the system properties when the structure is subjected to a prescribed seismic excitation, the parameters that define the model of Figure 1 are taken to be random with triangular probability distribution with mode at their best estimate value and the lower and upper bounds defined in Table 3.

The best estimate of f_y was calculated with the SCT-85 spectrum for ductility 4. The fixed-base period was used in this calculation for the fixed-base and the SSI

Table 4. Effect of system properties variability on ductility demand

period (sec)	best estimate	mean	σ
Fixed-Base			
0.4	3.8	5.9	9.7
1.2	4.0	2.9	1.1
2.0	4.0	3.7	0.8
2.8	4.0	3.8	0.7
3.6	3.9	4.0	0.7
SSI Case A			
0.4	3.4	4.0	5.6
1.2	4.3	4.4	1.0
2.0	5.5	4.5	0.9
2.8	5.9	5.3	1.3
3.6	5.7	5.3	1.3
SSI Case B			
0.4	19.0	8.0	8.7
1.2	4.1	3.8	0.8
2.0	3.0	3.3	0.5
2.8	3.8	3.4	0.8
3.6	3.6	3.0	0.9

case B systems. The SSI period T^* was used for the SSI case A systems. Note that all the probability distributions are symmetric with the exception of that for f_y , which is biased toward the higher values.

The analysis follows several steps. First, particular values for the system properties are generated by Monte Carlo simulation using their corresponding probability distributions. 900 SSI systems were obtained for each fixed-base period. Each of these systems was analyzed using as input the SCT-85 record. Mean values and standard deviations of the ductility demand and the interstorey drift were calculated subsequently.

Mean ductility demands are shown on Figure 9. Results for selected periods also are listed in Table 4. For the fixed-base case the mean values are very close to the target ductility of 4, with the exception of $T = 0.4s$, which yield values close to 6. In general, for SSI case A systems, the mean ductility demand is higher than both the design value of 4, and the demand for the fixed-base case. The explanation is that the SCT-85 spectrum for ductility 4, used to calculate the best estimate of f_y , tends to decrease with increasing periods. Therefore the f_y corresponding to the SSI period are, in general, smaller than for the fixed-base period.

Figure 10 compares mean ductility demands with the results obtained using best estimate (BE) properties, for SSI case A systems. This figure and Table 4 show that the mean ductilities are, in general, smaller than the BE values for all periods except 0.4s and 1.2s. The differences, however, are not significant. Figure 10 also depicts the mean ductility demands plus one standard deviation. The dispersions are relatively large for small periods, and significantly smaller and uniform

for periods longer than 1.2s.

Figure 11 shows mean interstory drifts for the three design cases. Again, selected results are presented in Table 5. In general, the inclusion of SSI increases the interstory drift for periods smaller than 1.6s and causes a reduction for longer periods. The differences, however, are not significant. Peak interstory drifts occur at $T = 2s$ for fixed-base systems and $T = 1.6s$ for SSI systems (note that this last value of T corresponds to an SSI period of $1.25 \times 1.6 = 2s$). This range of periods coincide with the dominant periods of the SCT-85 record as illustrated by the elastic spectra on Figure 2.

Table 5. Effect of system properties variability on interstory drift (times 10^{-3})

period (sec)	SCT-85	mean	σ
Fixed-Base			
0.4	2.4	3.9	6.0
1.2	8.0	6.3	2.0
2.0	10.3	10.8	2.1
2.8	6.2	6.7	1.1
3.6	4.4	4.8	0.4
SSI Case A			
0.4	2.3	2.8	3.4
1.2	7.8	8.7	1.6
2.0	11.0	9.7	1.0
2.8	5.9	5.7	0.8
3.6	3.3	3.4	0.5
SSI Case B			
0.4	12.2	5.2	5.1
1.2	8.2	8.3	1.6
2.0	9.0	9.6	1.4
2.8	6.0	5.9	0.7
3.6	4.0	3.5	0.7

Figure 12 is a comparison of mean interstory drifts with mean values plus one standard deviation and with the BE results, for SSI case A models. The mean values are remarkably close to the BE results for all periods. Table 5 shows the same pattern for fixed-base and SSI case B systems. The standard deviations are noticeable for periods smaller than 1.6s, and remain small and uniform for longer periods.

Additional cases have been analyzed considering one of the properties listed in Table 3 as deterministic and keeping the rest of them random. The most significant changes in the seismic response statistical parameters resulted when f_y was changed from random to deterministic. Figure 13 compares mean ductility demands for both situations for fixed-base and SSI case A systems. The mean ductilities for random f_y are smaller than those for deterministic f_y because the distribution of this property is biased towards values

higher than the best estimate. A similar comparison is presented in Figure 14 for mean interstory drifts. The differences follow the same pattern, although they are not as significant as for ductility demands.

Frequently, structures with short periods are overdesigned. To have a quantitative idea of the impact that this could have on the seismic response, we have reanalyzed the fixed-base system for $T=0.4s$, considering f_y 10 percent greater than the value calculated with the spectral ordinate. The mean and the standard deviation of the ductility demand were reduced from 5.89 and 9.74 (Table 4) to 1.96 and 3.37, respectively. Reductions of similar magnitude occur for the interstory drift, showing that overdesign is a factor that deserves additional consideration.

5 CONCLUSIONS

A statistical analysis of the variability of seismic response of fixed-base and soil-structure interaction systems due to uncertainties in the input ground motion and in the system dynamic properties has been presented. The results indicate that significant dispersions appear in ductility demands, particularly for relatively small periods, as a result of both sources of uncertainty. The dispersions, however, are not as noticeable for interstory drifts. This underscores the importance of studying simultaneously different measures of the seismic response.

The results for both fixed-base and SSI systems show that in many instances mean ductility demands were greater than the ones obtained following conventional design procedures which use best estimate properties and a "mean" design spectrum. This was particularly the case for short periods. In general, the standard deviation of the response is also significantly greater for short periods. In all the cases considered here, the variability of the yield strength has a strong effect on the variability of ductility demands and peak displacements. It is, therefore, necessary to evaluate whether current design practices with a smoothed spectrum (rather than the SCT-85 spectrum) and with actual strengths larger than the nominal ones, provide a more adequate and uniform safety margin.

In general, soil-structure interaction increases the mean peak response for short and medium fixed-base periods (say smaller than 2 seconds). For longer periods, the interaction reduces the mean response. The randomness in the soil-structure interaction parameters can, in some instances, increase significantly the standard deviation of the response, and, consequently, the probability of exceeding extreme values.

6 ACKNOWLEDGMENTS

We thank Sonia E. Ruiz of the National University of Mexico (UNAM) for providing the synthetic records used in this study. This work was sponsored by the National Science Foundation under Grants No. BCS-9116089 and BCS-9020394; Dr. H. J. Lagorio is the program cognizant official. We are grateful for this support.

REFERENCES

- Grigoriu, M., S.E. Ruiz & E. Rosenblueth 1988. *Nonstationary Models of Seismic Ground Acceleration*. *Earthquake Spectra* 4-3: 551-568.
- Gumbel, E. J. 1958. *Statistics of Extremes*. New York: Columbia University Press.
- Jennings, P.C., & J. Bielak 1973. Dynamics of Building-Soil Interaction. *Bulletin of the Seismological Society of America* 63 (1): 9-48.
- Reglamento de Construcciones para el Distrito Federal 1987. *Gaceta Oficial del Departamento del D.F.*, 6 de Julio. Mexico: Mexico D.F. (in Spanish).

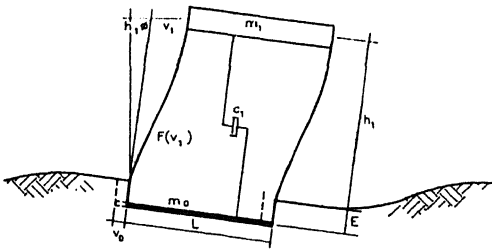


FIG. 1 BUILDING FOUNDATION SYSTEM

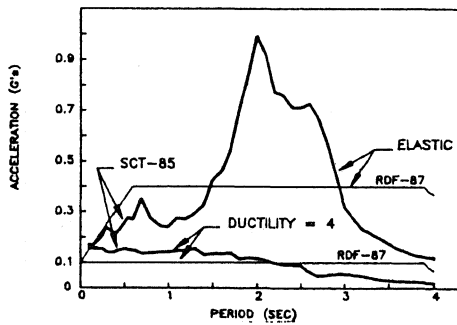


FIG. 2 ELASTIC AND INELASTIC SPECTRA
SCT-85 RECORD AND RDF-87

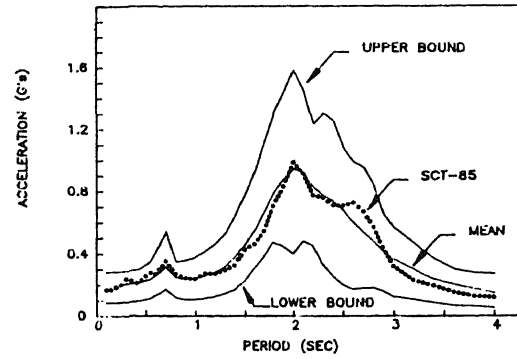


FIG. 3 PSEUDOACCELERATION SPECTRA,
SCT-85 AND SYNTHETIC RECORDS

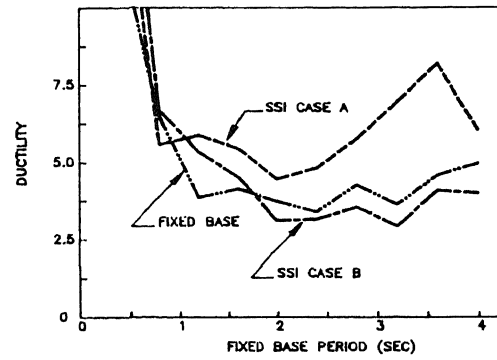


FIG. 4 MEAN DUCTILITY DEMAND FOR
SYNTHETIC EARTHQUAKES

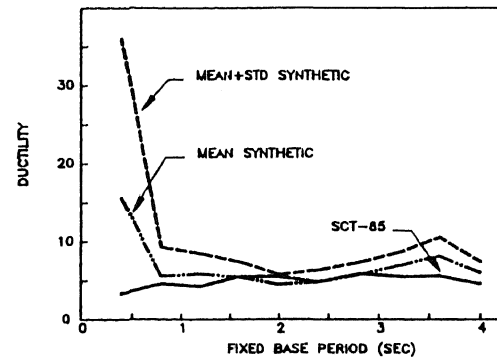


FIG. 5 DUCTILITY DEMAND, SSI CASE A

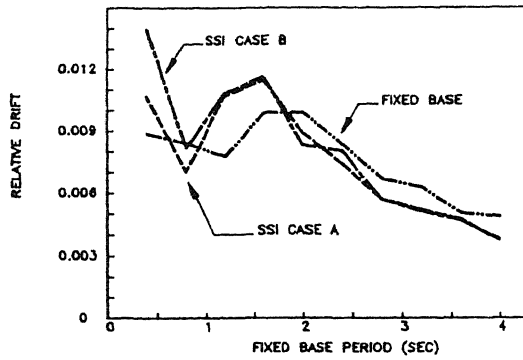


FIG. 6 MEAN INTERSTORY DRIFT

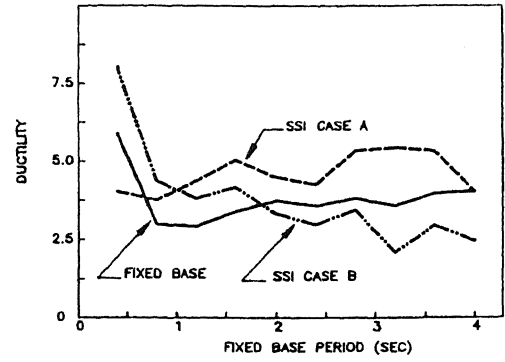


FIG. 9 MEAN DUCTILITY DEMAND FOR PROBABILISTIC SYSTEM PROPERTIES

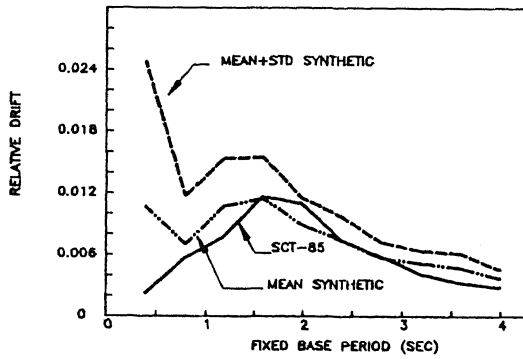


FIG. 7 RELATIVE DRIFT, SSI CASE A

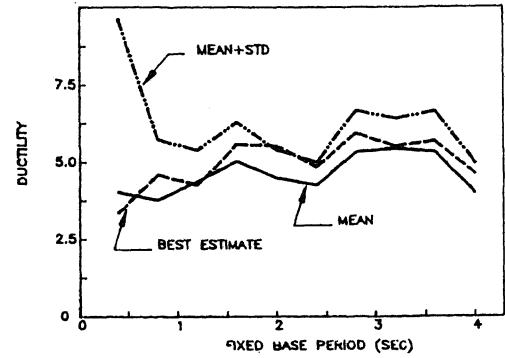


FIG. 10 DUCTILITY DEMAND, SSI CASE A FOR PROBABILISTIC SYSTEM PROPERTIES

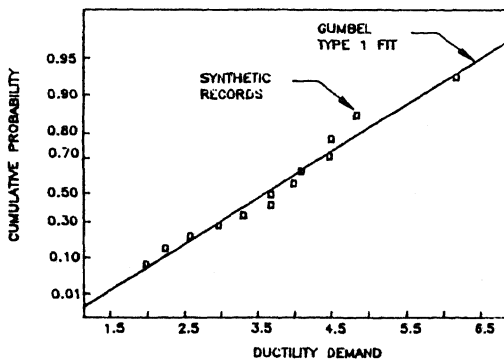


FIG. 8 DUCTILITY PROBABILITY DISTRIBUTION
FIXED BASE CASE, T = 2 SECONDS

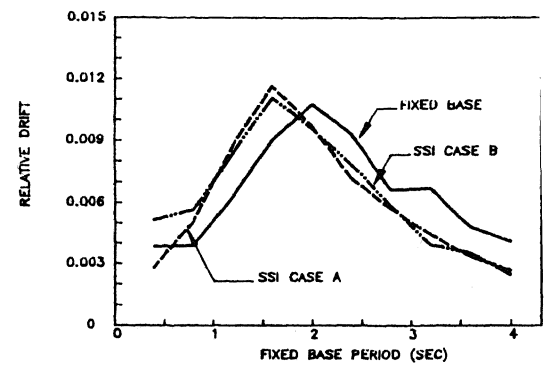


FIG. 11 MEAN INTERSTORY DRIFT FOR PROBABILISTIC SYSTEM PROPERTIES

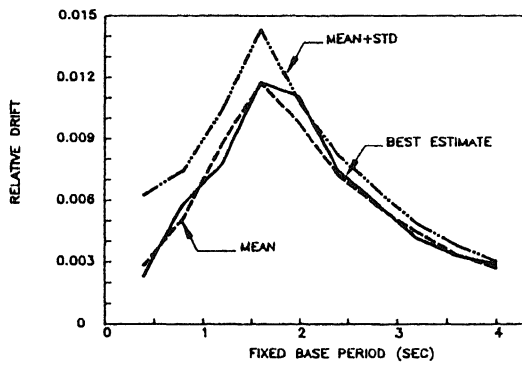


FIG. 12 MEAN INTERSTORY DRIFT, SSI CASE A

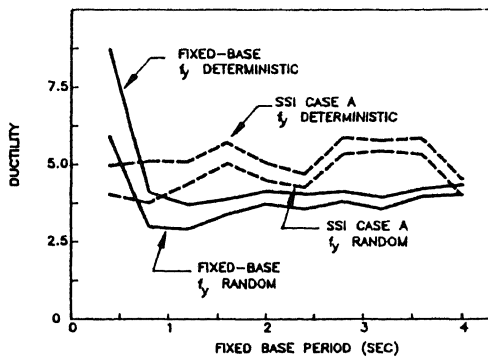


FIG. 13 EFFECT OF VARIABILITY OF f_y ON MEAN DUCTILITY DEMAND

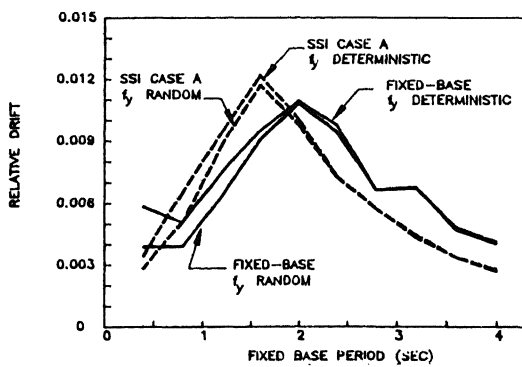


FIG. 14 EFFECT OF VARIABILITY OF f_y ON MEAN INTERSTORY DRIFT

